energy&fuels

Article

pubs.acs.org/EF

Dry De-NO_x Process via Gas-Phase Photochemical Oxidation Using an Ultraviolet and Aerosolized H_2O/H_2O_2 Hybrid System

Jeongan Choi,[†] Kang Soo Lee,[†,‡] Dong Yun Choi,[†] Yong Jin Kim,[§] and Sang Soo Kim*[,†]

[†]Aerosol and Particle Technology Laboratory, Department of Mechanical Engineering, Korea Advanced Institute of Science and Technology, 291 Daehak-ro, Yuseong-gu, Daejeon 305-701, South Korea

[‡]Ralph M. Parsons Laboratory, Department of Civil and Environmental Engineering, Massachusetts Institute of Technology, 77 Massachusetts Avenue, Cambridge, Massachusetts 02139, United States

[§]Eco-Machinery Division, Korea Institute of Machinery and Materials, 156 Gajeongbuk-ro, Yuseong-gu, Daejeon 305-343, South Korea

Supporting Information

ABSTRACT: A dry de-NO_x technique based on a highly efficient photochemical oxidation process was demonstrated for a simulated flue gas of a diesel engine using a lab-scale reaction chamber. A hybrid system of an ultraviolet ($UV_{185,\ 254\ nm}$) lamp and aerosolized H_2O/hydrogen peroxide (H_2O_2) was employed. De-NO_x characteristics when using an UV lamp, an aerosolized H_2O/H_2O_2 solution, and a hybrid system of both components were investigated individually. The UV lamp treatment had a significant impact on the de-NO_x process by generating ozone, while the aerosolized H_2O/H_2O_2 solution showed less effect because of the ambient temperature when the system was operated separately. With the assistance of UV light, however, aerosolized H_2O/H_2O_2 contributed to the oxidation reaction and NO and NO_2 removal efficiencies of up to 100 and 97.8%, respectively, were achieved. Ammonia was introduced into the reaction chamber to solidify and remove the oxidized nitric oxide (NO) through the formation of ammonium nitrate aerosols. Scanning electron microscopy and energy-dispersive spectroscopy analysis were used to identify and interpret the particulate byproducts after the reaction.

1. INTRODUCTION

Over recent decades, NO_x has been regarded as an important pollutant with many adverse environmental and health effects; e.g., it has a role in global warming, smog, acid rain, ozone destruction, and the incidence of respiratory diseases.[1] Strict regulations of NO_x emissions from diesel engines, such as the European emission standards, have been legislated.[2] Currently, the regulation of heavy-duty diesel engines, which are used for large vessels or power plants, is weak compared to that for light-duty vehicles.[3] However, the regulation of heavy-duty diesel engines will undoubtedly be tightened as environmental and health concerns continue to grow.

Many technologies have been proposed to meet the strict regulations on NO_x emission, e.g., exhaust gas recirculation (EGR) and several injection techniques.[4,5] Even though these technologies can be operated without extra facilities, the de-NO_x efficiency is too low to meet the upcoming regulation criteria. To address this issue, several after-treatment systems, such as selective catalytic reduction (SCR) or selective non-catalytic reduction (SNCR), have been employed. SCR has been widely used because it has a higher de-NO_x efficiency than SNCR.[6] However, it requires not only expensive installation costs but also rigid operating conditions.[7,8] Although many other technologies (e.g., discharging, plasma treatment, electron beam irradiation, and adsorption and scrubbing processes) have been developed to address these shortcomings, the performance of these systems is not yet sufficient to replace SCR.[9−13]

Recently, an advanced oxidation treatment technique using a hybrid system of an ultraviolet (UV) lamp and hydrogen peroxide (H_2O_2) was introduced in coal-fired power plants.[14] The oxidation of nitric oxide (NO) by H_2O_2 injection generally takes place at relatively high temperatures (~700 °C).[15−17] In contrast, when the UV lamp and H_2O_2 hybrid system is employed, oxidation will occur even at room temperature by virtue of the UV lamp.[18,19] The UV lamp generates OH, H, O, and HO_2, which are readily oxidized.[19] Because of its intrinsically simple and sustainable characteristics, this technique is considered to be a promising after-treatment technology. It has also been applied to wastewater purification and the treatment of pollutants from fabric-dying processes.[20−22] However, for wider use, the issue of low NO oxidation and removal efficiency (70−80%) must be overcome.[14] Also, the UV/H_2O_2 hybrid system usually has been operated in a wet process. After-treatment techniques for gaseous pollutants are mainly classified into two categories: dry and wet methods. Although wet techniques have been widely used because of their high removal efficiencies for most gaseous pollutants (e.g., SO_x and heavy metals), they cannot be directly applied to NO removal because NO is rarely soluble in a wet absorbent.[23] Instead, NO is first converted into nitric dioxide (NO_2) and then eliminated using a wet scrubber. In general, the ratio of NO/NO_2 in the flue gas from a diesel engine is approximately 9:1.[24] Therefore, the rate of conversion from NO to NO_2 is one of the most important factors determining the efficiency of a wet de-NO_x process. The purification of the wastewater produced during a wet de-NO_x process is another

Received: March 23, 2014
Revised: July 15, 2014
Published: July 15, 2014

   dx.doi.org/10.1021/ef500645a | Energy Fuels 2014, 28, 5270−5276

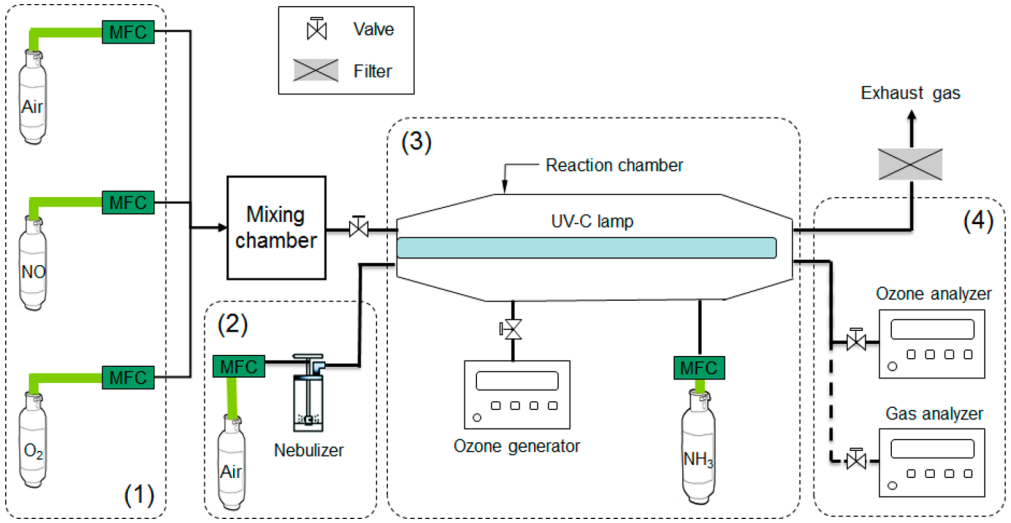

Figure 1. Schematic of the experimental setup: (1) generation of simulated flue gas, (2) nebulizer system that aerosolizes the aqueous H_2O_2 solution, (3) UV lamp-equipped reaction chamber, and (4) measurement devices.

issue to consider when designing an environmentally sustainable system configuration.

In this study, a dry removal process for NO and NO_2 removal using a hybrid system based on an UV lamp and aerosolized H_2O/H_2O_2 was demonstrated. The hybrid system achieved both a high NO_x removal efficiency and an environmentally sustainable treatment process. The characteristics of each component were evaluated, and thereafter, the hybrid system was investigated. Most studies on photochemical oxidation have been conducted using an UV lamp with a peak wavelength of 254 nm.[7,14,21] We used an UV lamp with two different peak wavelengths: 185 and 254 nm. Ozone was generated by radiation at 185 nm, which directly improved the oxidation of NO as well as NO_2 removal. Aerosolized H_2O/H_2O_2 was converted into H and OH radicals by exposure to $UV_{185,\ 254\ nm}$ radiation. A high removal efficiency was achieved through the operation of the advanced oxidation process (AOP) at room temperature. Production of a waste solution, including nitric acid (HNO_3), could be prevented by the application of an aqueous H_2O_2 solution.

2. MATERIALS AND METHODS

2.1. Experimental Apparatus. Figure 1 shows a schematic diagram of the experimental setup consisting of four sections: (1) the generation of a simulated flue gas, (2) a nebulizing system that aerosolizes H_2O/H_2O_2, (3) a UV lamp-equipped reaction chamber, and (4) measurement devices. In addition, an ozone generator was also used alongside the UV lamp.

The flue gas of a heavy-duty diesel engine was simulated by mixing different gas species: air, oxygen, and NO (0.2% NO with 98.8% N_2 balanced). The flow rate of each gas was regulated via a mass flow controller (MFC, FC-280SAV, Mykrolis, Billerica, MA), and the NO concentration in the carrier gas was adjusted by controlling the mixing ratio between each gas. To ensure the uniformity of the mixed gas, a mixing chamber was installed between the gas generation section and the reaction chamber. The relative humidity and temperature of the simulated flue gas were 20% and 25 °C, respectively.

The H_2O/H_2O_2 solution was aerosolized by a Collison nebulizer (six jets, BGI Co., Waltham, MA) and injected into the reaction chamber to enhance the degree of dispersion as well as to lower substantially the solution usage compared to conventional liquid−gas reactions, i.e., wet slurry and bubble reactors. The mixing ratio was adjusted from 10:0 to 7:3 (H_2O/H_2O_2), and micron-sized aerosols were generated by collisions between the solution and the nebulizer bottle wall.[25] Aerosolized H_2O/H_2O_2 comprised only a small portion of the flue gas and was either decomposed in the reaction or evaporated immediately.

The 56 cm long reaction chamber was made of poly(methyl methacrylate) (PMMA) and had a circular cross-section (inner diameter of 9.0 cm and outer diameter of 9.5 cm). A cylindrical quartz pipe (inner diameter of 2.3 cm and length of 55 cm) was placed at the center of the reaction chamber, and a UV-C lamp (G24T5VH, Hansung Ultraviolet Co., Ltd., Korea; power = 25 W) was installed inside the quartz pipe. The UV-C lamp produced two different peak wavelengths: 185 and 254 nm (see the Supporting Information for the output data of the UV-C lamp). Ozone and OH were produced at each wavelength, respectively. To solidify the reacted and converted pollutants (e.g., NO_2 and HNO_3) into ammonium nitrate (NH_4NO_3) powder, which is a chemically neutral byproduct that can be recycled as an agricultural fertilizer, gaseous NH_3 was injected into the reaction chamber. An ozone generator (LAB-S, Ozonetech Co., Korea) was placed in the reaction chamber to enable the influence of ozone generated by the UV-C lamp on the oxidation characteristics to be assessed.

NO and NO_x in the exhaust gas were measured in real time using a gas analyzer (PG-250, Horiba Co., Japan), and the ozone concentration was monitored with an ozone analyzer (UV-100, Eco Sensors Co., Santa Fe, NM). Concentrations of NO and NO_x were measured individually, and the NO_2 concentration was calculated by subtracting the NO concentration from the NO_x concentration. To identify and characterize the morphology of the solid-state byproduct after reaction (i.e., NH_4NO_3), particulate matter in the exhaust gas was collected on glass microfiber filter papers with a 1.2 μm pore size (Whatman Co., U.K.) because the converted particles had a size distribution of 2.5−10 μm.[26] The particles were observed using field emission scanning electron microscopy (FE-SEM, Sirion, FEI Co., Netherlands) and chemically analyzed by energy-dispersive spectroscopy (EDS).

2.2. Experimental Procedure. In this study, experiments were performed step by step. The characteristics of the de-NO_x process using either an UV lamp or aerosolized H_2O/H_2O_2 were investigated individually. Thereafter, a hybrid system using both components was examined.

Flue gas with 400 ppm of NO was simulated and injected into the reaction chamber. The flow rate was controlled to within 1−6 L/min to adjust the UV lamp power exerted per unit volume of carrier gas. NH_3 was injected with the same molar concentration of NO. To determine the contribution of ozone generated by the UV lamp on the oxidation process, ozone was generated by the ozone generator at the same concentration produced by the UV lamp, and the de-NO_x

dx.doi.org/10.1021/ef500645a | Energy Fuels 2014, 28, 5270−5276

characteristics of the two different methods were compared to each other. The effect of the NH_3 on the de-NO_x process was investigated by comparing the results with or without NH_3. The removal efficiency was calculated by

$$\eta = \frac{C_{inlet} - C_{outlet}}{C_{inlet}} \times 100\% \quad (1)$$

where C_{inlet} and C_{outlet} are NO_x concentrations at the inlet and outlet, respectively.

To characterize the de-NO_x process by the aerosolized H_2O/H_2O_2 treatment, an aqueous H_2O_2 solution (H_2O/H_2O_2 = 7:3) was aerosolized using a Collison nebulizer. Table 1 shows the aerosolized liquid volume in terms of a gas flow rate injected into the nebulizer. The amount of aerosolized liquid was adjusted from 2.5 to 6.5 mL/h by controlling the air flow rate into the nebulizer from 1.5 to 6.0 L/min, while the flow rate of the flue gas was fixed to 5 L/min.

Table 1. Usage Rate of Aqueous H_2O_2 Solution by the Collison Nebulizer

inlet flow rate (L/min)	liquid use rate (mL/h)
1.5	2.5
3	3.6
4.5	5
6	6.5

To assess the de-NO_x efficiency of the UV lamp and aerosolized H_2O/H_2O_2 hybrid system, the UV lamp was turned on and H_2O/H_2O_2 aerosol was generated with an air flow rate into the nebulizer of 5 L/min (amount of aerosolized solution of 5.5 mL/h). NH_3 as a neutralizing agent was also injected into the reaction chamber at the same molar concentration as NO. The flow rate of the simulated flue gas was maintained between 1 and 6 L/min. The UV irradiation intensity was controlled by adding or removing UV lamps, and the H_2O_2 concentration in the aqueous solution was adjusted to be within 0−30% to quantify the effect of UV irradiation intensity and H_2O_2 on the de-NO_x process.

3. RESULTS AND DISCUSSION

3.1. NO_x Removal by the UV Lamp. The UV lamp de-NO_x process used ozone generated by the UV lamp, especially at the 185 nm wavelength. The ozone generation procedure is as follows:[27]

$$O_2 + h\nu\ (185\ nm) \rightarrow O + O \quad (2)$$

$$O_2 + O \rightarrow O_3 \quad (3)$$

Subsequently, the de-NO_x process by ozone is

$$NO + O_3 \rightarrow NO_2 + O_2 \quad (4)$$

$$NO_2 + O_3 \rightarrow NO_3 + O_2 \quad (5)$$

$$NO_2 + H_2O \rightarrow HNO_3 + {}^{\bullet}H \quad (6)$$

$$NO_3 + {}^{\bullet}H \rightarrow HNO_3 \quad (7)$$

Figure 2 shows the de-NO_x characteristics of the UV lamp treatment. The NO concentration at the inlet of the reaction chamber was set to 400 ppm. As the flow rate increased from 1 to 6 L/min, the NO and NO_x concentrations at the outlet increased from 73.8 and 145 ppm to 246.5 and 265.4 ppm, respectively, and the calculated removal efficiencies decreased from 81.55 and 63.75% to 38.37 and 33.65%, respectively, which was attributable to the reduction of the UV exposure time on the unit gas volume because of the increased flow rate. The reaction times in the reaction chamber were 214 and 35.6 s for the flow rates of 1 and 6 L/min, respectively. As shown in Figure 2a, the trend in the NO_2 concentration in terms of the flow rate indicates a peak value for a flow rate of 2 L/min, which was due to the NO oxidation rate being larger than the NO_2 elimination at a flow rate below 2 L/min. As the flow rate increased beyond 2 L/min, the conversion rate from NO to NO_2 decreased gradually and the total concentration of NO_2 declined accordingly. In this experiment, a high NO removal efficiency was achieved by the UV lamp treatment. Ozone was a suitable reactant for the oxidation method because ozone generated by UV irradiation was stable and could be sustained for much longer than other oxidation radicals.[28]

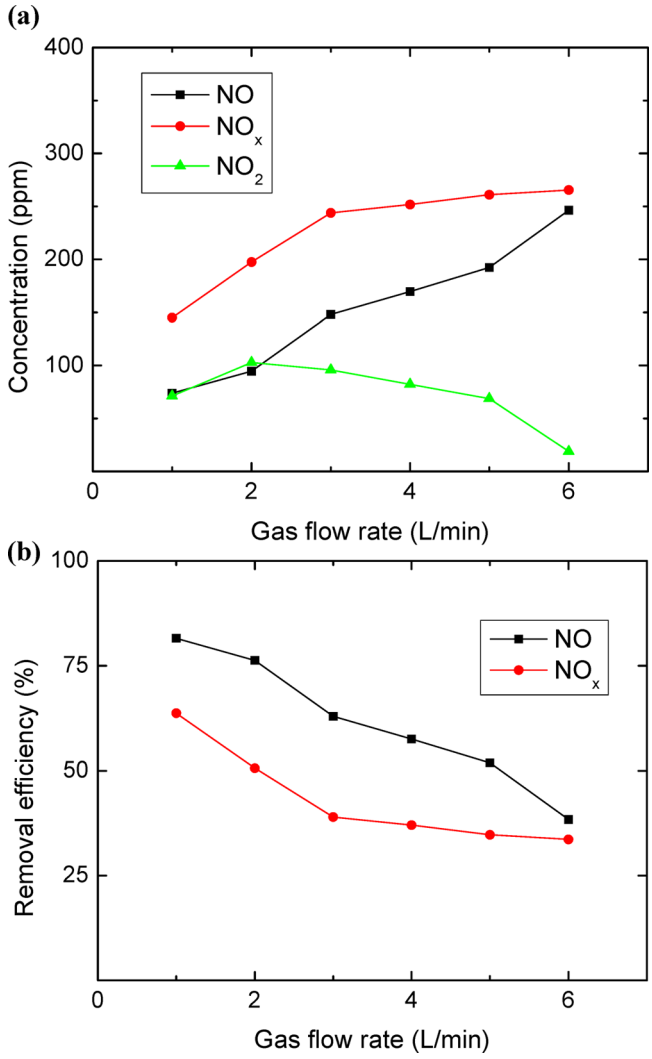

Figure 2. De-NO_x characteristics of the UV lamp treatment: (a) concentration of NO, NO_2, and NO_x in terms of the gas flow rate and (b) removal efficiencies of NO and NO_x. Conditions: concentration of NO, 400 ppm; concentration of NH_3, 400 ppm; UV lamp power, 25 W; and reaction temperature, 25 °C.

Figure 3a shows the characteristics of ozone generation by the UV lamp in terms of reaction time and the used gas species. In air, as the reaction time increased from 80 to 800 s, the ozone concentration varied from 105 to 404 ppm. It was approximately 3 times higher in oxygen because no UV energy was used by nitrogen; the ozone concentrations were 341 and 1100 ppm for the reaction times of 80 and 800 s, respectively. To further assess the de-NO_x process via ozone generated by the UV lamp, the removal characteristics through ozone

dx.doi.org/10.1021/ef500645a | Energy Fuels 2014, 28, 5270−5276

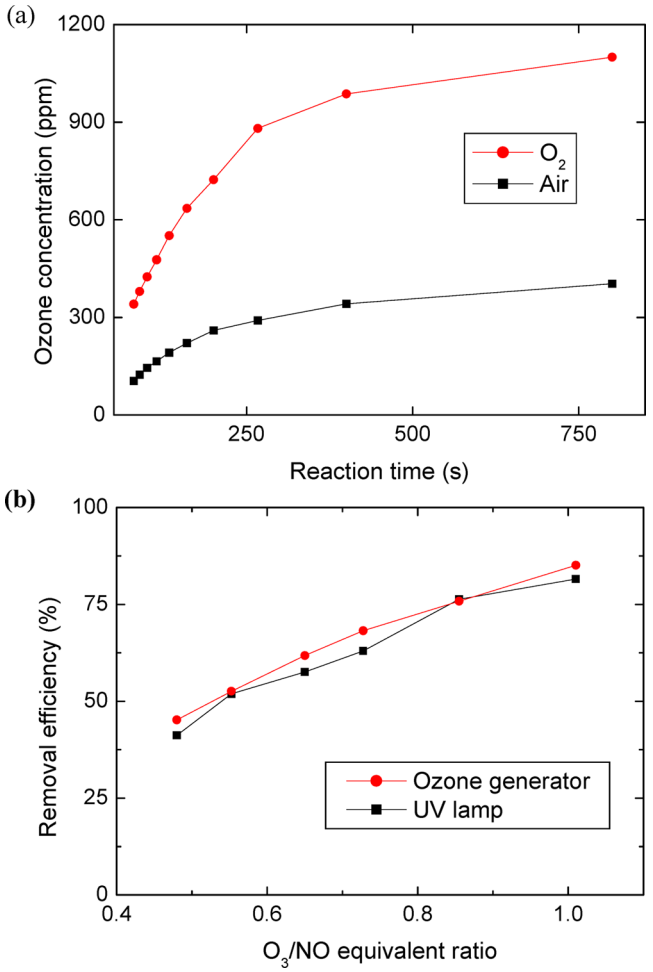

Figure 3. Comparison of de-NO_x efficiency between two different ozone generation systems: (a) ozone generation by UV lamp and (b) NO removal efficiencies by either an UV lamp or a conventional ozone generator. Conditions: concentration of NO, 400 ppm; concentration of NH_3, 400 ppm; UV lamp power, 25 W; and reaction temperature, 25 °C.

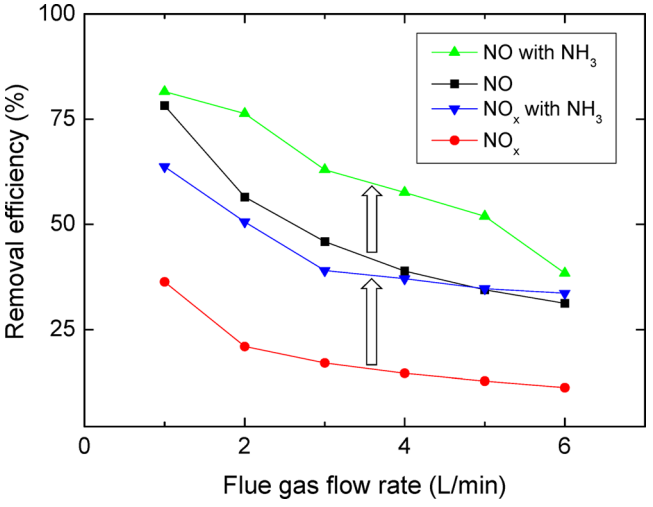

Figure 4. Effect of NH_3 injection on the UV lamp-induced de-NO_x process in terms of the flow rate of flue gas. Conditions: concentration of NO, 400 ppm; concentration of NH_3, 400 ppm; UV lamp power, 25 W; and reaction temperature, 25 °C.

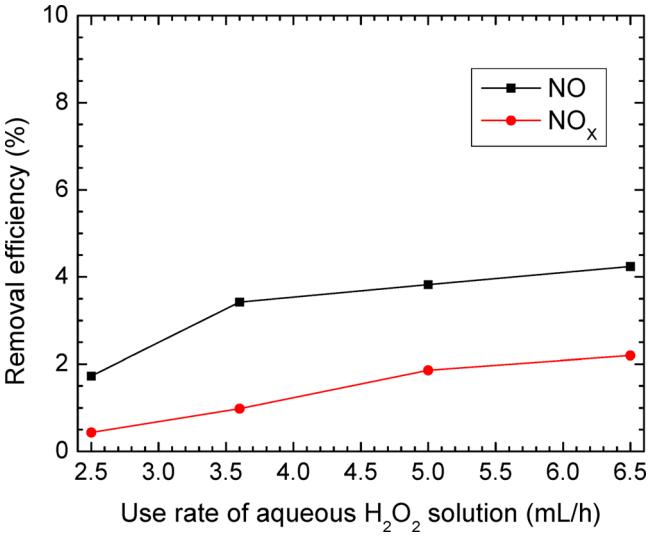

Figure 5. Characteristics of the de-NO_x process using aerosolized aqueous H_2O_2 solution under different rates of liquid usage. Conditions: concentration of NO, 400 ppm; flue gas flow rate, 5 L/min; solution, 30% H_2O_2 in water; and reaction temperature, 25 °C.

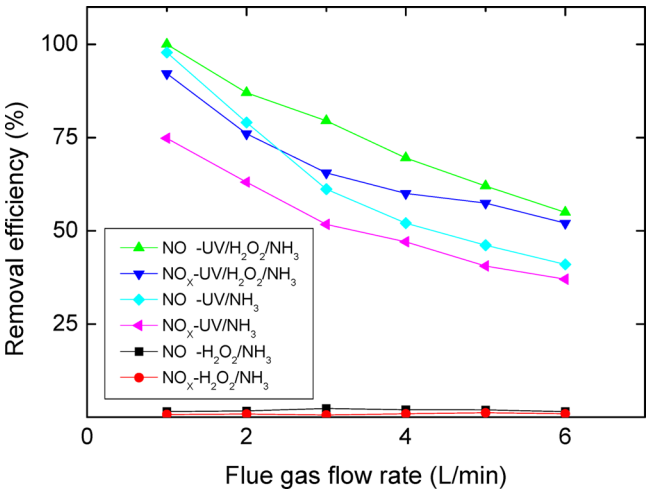

Figure 6. Comparison of de-NO_x efficiencies among three different system configurations: UV lamp, aerosolized aqueous H_2O_2 solution, and a hybrid system of both treatments. Conditions: concentration of NO, 400 ppm; concentration of NH_3, 400 ppm; UV lamp power, 25 W; 30% H_2O_2 solution use rate, 5.5 mL/h (nebulizer inlet flow rate, 5 L/min); and reaction temperature, 25 °C.

Table 2. Comparison of De-NO_x Efficiencies at Different UV Radiation Intensities[a]

UV intensity (W)	NO removal efficiency (%)	NO_x removal efficiency (%)
0	4	2
25	61.9	57.4
50	91.7	88

[a]Conditions: concentration of NO, 400 ppm; concentration of NH_3, 400 ppm; flue gas flow rate, 5 L/min; 30% H_2O_2 solution use rate, 5.5 mL/h; and reaction temperature, 25°C.

generated by either UV or a commercial ozone generator were evaluated. Figure 3b shows the NO removal efficiency as a function of the O_3/NO equivalent ratio. When the O_3/NO equivalent ratio was equal to 1.01, the removal efficiencies were 81.55 and 76.32% for the ozone generator and the UV lamp,

dx.doi.org/10.1021/ef500645a | Energy Fuels 2014, 28, 5270−5276

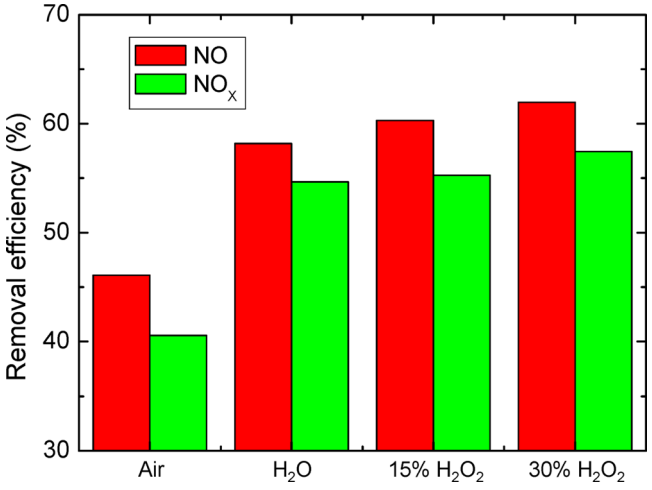

Figure 7. De-NO_x efficiency of the hybrid system in terms of the composition of the aerosolized solution. Conditions: concentration of NO, 400 ppm; concentration of NH_3, 400 ppm; UV lamp power, 25 W; nebulizer inlet flow rate, 5 L/min; and reaction temperature, 25 °C.

respectively. The corresponding values decreased to 47.6 and 41.2%, respectively, at an O_3/NO equivalent ratio of 0.48. The results from the two different systems are quite similar, which suggests that the other radicals produced by the UV lamp do not play an important role in the de-NO_x process. The slight difference (1−5%) may have been due to the oxidation mechanisms. The ozone generator produced ozone, which was then injected into the reaction chamber, while the UV lamp generated ozone within the reaction chamber. From the Beer−Lambert law,[7] NO in the reaction chamber was determined to hinder the UV light irradiation of oxygen molecules. As a result, the amount of ozone generated by the UV lamp was slightly lower than that produced by the ozone generator.

NH_3 was injected into the system at the same molar concentration as NO because it can effectively remove residual NO_x and ammonia gas. Excess NH_3 may induce hazardous health effects, e.g., irritation and the fatal malfunction of the eyes, nose, and throat.[29] Figure 4 shows the removal efficiencies of NO and NO_x with or without NH_3 injection, respectively. The nebulizer was turned off for this experiment. Both removal efficiencies were inversely proportional to the flow rate of the flue gas. When the flow rate was 1 L/min, the removal efficiencies of NO and NO_x were either 78.2 and 36.3% without NH_3 or 81.5 and 63.75% with NH_3, respectively. When the flow rate increased to 6 L/min, the removal efficiencies decreased to either 31.2 and 11.2% without NH_3 or 38.4 and 33.7% with NH_3, respectively, because of the reduction in UV irradiation time. The magnitude of the improvement in the removal efficiency was greater for NO_x (NO + NO_2) than NO. Typically, the NO removal efficiency with NH_3 was similar to that without NH_3 at both high and low flow rates. The initial molar ratio of O_3/NO varied from 1.01 to 0.48 for flow rates between 1 and 6 L/min. The effect of NH_3 injection on the NO removal efficiency was larger at higher O_3/NO (i.e., lower flow rates) because the back reaction (NO_2 → NO) was reduced. The generation of NH_4NO_3 according to the reaction between NH_3 and HNO_3 could improve the oxidation of NO.[28] Therefore, NO removal efficiencies with and without NH_3 were quite similar at the high flow rate. When the flow rate was low enough, NO removal efficiencies with and without NH_3 were also similar because of the large NO oxidation rate with ozone.

The formation of NH_4NO_3 is relevant to the improvement of the NO and NO_x removal efficiencies.[28] NO_x from reactions 6 and 7 is removed through the formation of NH_4NO_3.[26,28]

$$HNO_3 + NH_3 \rightarrow NH_4NO_3 \quad (8)$$

UV-induced oxygen atoms reduce the NO oxidation rate because of a reverse reaction.[28,30]

$$NO_2 + O \rightarrow NO + O_2 \quad (9)$$

Therefore, the less that the reverse reaction 9 takes place, the more NO is removed. The difference in the NO_x removal efficiency between treatments with or without the injection of NH_3 is approximately 20−30%.

3.2. NO_x Removal by Aerosolized H_2O/H_2O_2. The droplet size distribution characterized by the mass median diameter (MMD) of the aerosolized H_2O/H_2O_2 mixture by the Collison nebulizing system was 2−3 μm.[31] Experimentally, a 10 μm water droplet has a life span of less than 1 s at 20 °C and 80% relative humidity.[25] As the aerosolized droplet diameter becomes smaller, the specific surface area increases, resulting in rapid evaporation. Moreover, because the vapor pressure of an aerosolized droplet depends upon the attractive force between neighboring molecules, fewer molecules at the surface of the

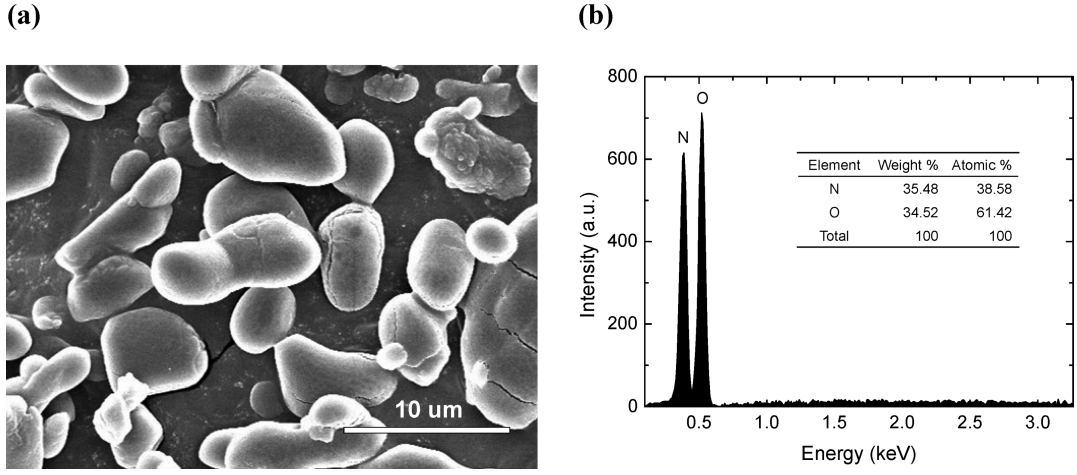

Figure 8. (a) SEM image of the particulate byproduct at a magnification of 3000× and (b) EDS spectrum.

dx.doi.org/10.1021/ef500645a | Energy Fuels 2014, 28, 5270−5276

large curvature of a small droplet can attain a high vapor pressure, as compared to a water droplet with a plane surface (i.e., a large droplet with small curvature).[32]

In this study, most aerosolized H_2O/H_2O_2 had a diameter of less than 3 μm and the rate of use of the aqueous H_2O_2 solution was so small that the droplets tended not to be agglomerated but evaporated rapidly in the reaction chamber. Figure 5 shows the NO and NO_x removal efficiencies in terms of the amount of aerosolized aqueous H_2O_2 solution (H_2O/H_2O_2 = 7:3). The reactions between NO_x and H_2O/H_2O_2 in a dry system are[14,33]

$$2NO + 3H_2O_2 \rightarrow 2HNO_3 + 2H_2O \quad (10)$$

$$NO_2 + H_2O_2 \rightarrow NO_3 + H_2O \quad (11)$$

$$4NO + O_2 + 2H_2O \rightarrow 4HNO_2 \quad (12)$$

$$2NO_2 + H_2O \rightarrow HNO_2 + HNO_3 \quad (13)$$

The de-NO_x process by H_2O/H_2O_2 treatment occurs at much higher temperatures (~700 °C) than room temperature.[15,16] As shown in Figure 5, the removal efficiencies of both NO and NO_x are close to zero because the surrounding temperature is too low to activate the reactions between NO_x and H_2O_2. Aerosolized H_2O is also not effective for NO removal because NO has very low solubility in H_2O. Considering the fact that NO_x is unstable, a very slight effect of the H_2O/H_2O_2 treatment on the removal efficiency is plausible: the removal efficiencies of NO and NO_x were 4.2 and 2.2%, respectively, when an aqueous H_2O_2 solution of 6.5 mL/h was aerosolized. The following subsection describes how UV irradiation was used to activate the reaction by H_2O/H_2O_2 at room temperature.

3.3. NO_x Removal by the UV and Aerosolized H_2O/H_2O_2 Hybrid System. Figure 6 shows the NO and NO_x removal efficiencies for three different system configurations as a function of the flow rate of carrier gas: UV lamp, aerosolized aqueous H_2O_2 solution, and a hybrid system of both treatments. With the UV and aerosolized aqueous H_2O_2 hybrid system, NO and NO_x removal efficiencies were 100 and 97.8% at a flow rate of 1 L/min, respectively, and 54.9 and 52% at a flow rate of 6 L/min, respectively. The removal efficiency of the hybrid system was higher than the sum of the two removal efficiencies produced by each individual component because the photoemission from the UV lamp produces free radicals from aerosolized aqueous H_2O_2 solution by the following chemical reactions:[27,34,35]

$$H_2O + h\nu\ (185\ nm) \rightarrow {}^{\bullet}OH + {}^{\bullet}H \quad (14)$$

$$H_2O_2 + h\nu\ (254\ nm) \rightarrow 2{}^{\bullet}OH \quad (15)$$

$UV_{254\ nm}$ diminishes ozone generation because of a reaction with water vapor in the flue gas that produces OH free radicals.[27]

$$O_3 + H_2O + h\nu\ (254\ nm) \rightarrow 2{}^{\bullet}OH + O_2 \quad (16)$$

The de-NO_x process by reaction with OH free radicals is[14]

$$NO + {}^{\bullet}OH \rightarrow NO_2 + {}^{\bullet}H \quad (17)$$

$$NO_2 + {}^{\bullet}OH \rightarrow HNO_3 \quad (18)$$

The O_3 and OH oxidation potentials are 2.07 and 2.8 V, respectively.[36] Because OH has a greater oxidation capability than ozone, OH contributes more to the oxidation power of this system. In comparison to the sum of the removal efficiencies of each individual component, the NO and NO_x removal efficiencies when using the hybrid system were enhanced by 7.9 and 23% at a flow rate of 1 L/min, respectively, and 13.9 and 25% at a flow rate of 6 L/min, respectively. In this study, only 5.5 mL/h of aqueous H_2O_2 solution was used. Because of the enhanced degree of solution dispersion, no liquid waste is produced in the reaction chamber and it achieves higher overall removal efficiencies.

Table 2 shows the NO and NO_x removal efficiencies in terms of different powers of UV irradiation (0, 25, and 50 W). NO and NO_x removal efficiencies of 91.7 and 88% were achieved with 50 W UV power and 5 L/min flue gas, respectively. While NO_x was effectively removed by increasing the power of UV irradiation, only about 4 and 2% of NO and NO_x could be removed by the aerosolized H_2O/H_2O_2 treatment alone, respectively.

Figure 7 shows the effect of the H_2O_2 concentration in the aqueous solution on the NO and NO_x removal efficiencies. The NO and NO_x removal efficiencies were 46 and 40%, respectively, when air was injected into the empty nebulizer without H_2O and H_2O_2. In general, H_2O has no influence on the de-NO_x process because NO_x is insoluble in H_2O. However, following the injection of H_2O in this system, the NO and NO_x removal efficiencies were enhanced by approximately 12 and 14%, respectively. This was because H_2O was converted into OH and H radicals by 185 nm UV radiation (eq 14) and the OH radical by 254 nm UV radiation (eq 16), which then participated in the removal reaction. A slight enhancement in the removal efficiency occurred with the injection of H_2O_2.

3.4. SEM and EDS Analyses of Byproducts. Figure 8 shows the SEM and EDS results of the byproduct aerosols, which were collected on filter paper after leaving the reaction chamber. The byproduct has a particle size smaller than 10 μm. Theoretically, the particle can be predicted to be NH_4NO_3 according to reaction 8. As seen in Figure 8b, the atomic ratio of the byproduct particle is 38.6:61.4 (N/O), which is a similar atomic ratio to that of NH_4NO_3. It is a colorless and odorless compound and can be produced by the ion-induced formation of heterogeneous nucleation in the reaction chamber.[37] This hybrid de-NO_x system is environmentally sustainable because it does not generate waste sludge and is a productive material that can be used as a fertilizer without any additional treatment.[26,38]

4. CONCLUSION

In this study, three different system configurations for a de-NO_x process were investigated and compared at the laboratory scale by considering several factors: flow rate of flue gas, NH_3 injection, UV lamp power, and H_2O_2 concentration in an aqueous solution. The ozone generated from the UV lamp was shown to play an important role in the de-NO_x process, and the oxidation characteristics following ozone generation from a UV lamp and ozone generator were quite similar. NH_3 used to solidify oxidized NO contributes to the removal of NO and NO_2. Aerosolized H_2O/H_2O_2 did not have a significant influence on the de-NO_x process because the low ambient temperature restricted the reaction between NO_x and the H_2O/H_2O_2 aerosol. However, with the assistance of an UV lamp, the H_2O/H_2O_2 solution contributes to the oxidation reaction by producing UV-induced free radicals. It is intrinsically environmentally sustainable because no liquid byproduct, such as HNO_3 solution, is generated, and it is highly efficient compared to the conventional design of an AOP because of the higher

dx.doi.org/10.1021/ef500645a | Energy Fuels 2014, 28, 5270−5276

degree of dispersion of H_2O/H_2O_2 aerosol, leading to a low rate of usage for the solution. NH_4NO_3 particles can be collected by one of the conventional systems [e.g., electrostatic participator (ESP)] and used as a fertilizer. The present system will also be simultaneously applicable to the removal of SO_x and heavy metals with a high oxidation potential.

■ ASSOCIATED CONTENT

Supporting Information

Spectrum of the UV-C lamp as provided by the manufacturer (Figure S1). This material is available free of charge via the Internet at http://pubs.acs.org.

■ AUTHOR INFORMATION

Corresponding Author

*Telephone: +82-42-350-3021. Fax: +82-42-350-3095. E-mail: sskim@kaist.ac.kr.

Notes

The authors declare no competing financial interest.

■ ACKNOWLEDGMENTS

This work was supported by a research project (De-NO_x Characteristics by Ozone and Soft X-rays) of the Korea Institute of Machinery and Materials and the BK21 Plus Program.

■ REFERENCES

(1) Man, C. K.; Gibbins, J. R.; Witkamp, J. G.; Zhang, J. *Fuel* **2005**, *84*, 2190−2195.
(2) European Union. Regulation (EC) No 595/2009. *Off. J. Eur. Union* **2009**, L188/1−L188/13.
(3) Johnson, T. V. *SAE Tech. Pap. Ser.* **2006**, DOI: 10.4271/2006-01-0030.
(4) Pradeep, V.; Sharma, R. P. *Renewable Energy* **2007**, *32*, 1136−1154.
(5) Zheng, M.; Reader, G. T.; Hawley, J. G. *Energy Convers. Manage.* **2004**, *45*, 883−900.
(6) Wendt, J. O. L.; Linak, W. P.; Groff, P. W.; Srivastava, R. K. *AlChE J.* **2001**, *47*, 2603−2617.
(7) Liu, Y.; Zhang, J.; Sheng, C.; Zhang, Y.; Zhao, L. *Energy Fuels* **2010**, *24*, 4931−4936.
(8) Wang, Z.; Zhou, J.; Zhu, Y.; Wen, Z.; Liu, J.; Cen, K. *Fuel Process. Technol.* **2007**, *88*, 817−823.
(9) Chien, T. W.; Chu, H. *J. Hazard. Mater.* **2000**, *B80*, 43−57.
(10) Deshwal, B. R.; Jin, D. S.; Lee, S. H.; Moon, S. H.; Jung, J. H.; Lee, H. K. *J. Hazard. Mater.* **2008**, *150*, 649−655.
(11) Zhao, G. B.; Garikipati, S. V. B. J.; Hu, X.; Argyle, M. D.; Radosz, M. *AlChE J.* **2005**, *51*, 1800−1812.
(12) Chang, J. S.; Urashima, K.; Tong, Y. X.; Liu, W. P.; Wei, H. Y.; Yang, F. M.; Liu, X. J. *J. Electrostat.* **2003**, *57*, 313−323.
(13) Chmielewski, A. G. *Radiat. Phys. Chem.* **2007**, *76*, 1480−1484.
(14) Liu, Y.; Zhang, J.; Sheng, C.; Zhang, Y.; Zhao, L. *Chem. Eng. J.* **2010**, *162*, 1006−1011.
(15) Collins, M. M.; Cooper, C. D.; Dietz, J. D.; Clausen, C. A.; Tazi, L. M. *J. Environ. Eng.* **2001**, *127*, 329−336.
(16) Kasper, J. M.; Clausen, C. A.; Cooper, C. D. *J. Air Waste Manage. Assoc.* **2012**, *46*, 127−133.
(17) Limvoranusorn, P.; Cooper, C. D.; Dietz, J. D.; Clausen, C. A.; Pettey, L.; Collins, M. M. *J. Environ. Eng.* **2005**, *131*, 518−525.
(18) Cooper, C. D.; Clausen, C. A.; Pettey, L.; Collins, M. M.; Fernandez, M. P. *J. Environ. Eng.* **2002**, *128*, 68−72.
(19) Greiner, N. R. *J. Chem. Phys.* **1966**, *45*, 99−103.
(20) Lucas, M. S.; Peres, J. A.; Puma, G. L. *Sep. Purif. Technol.* **2010**, *72*, 235−241.
(21) Arslan, I.; Balcioglu, I. A. *J. Chem. Technol. Biotechnol.* **2001**, *76*, 53−60.
(22) Modirshahla, N.; Behnajady, M. A. *Dyes Pigm.* **2006**, *70*, 54−59.
(23) Wu, Z.; Wang, H.; Liu, Y.; Jiang, B.; Sheng, Z. *Chem. Eng. J.* **2008**, *144*, 221−226.
(24) Willems, F.; Cloudt, R.; van den Eijnden, E.; van Genderen, M.; Verbeek, R.; De Jager, B.; Boomsma, W.; Van Den Heuvel, I. *SAE Int. Pap. Ser.* **2007**, DOI: 10.4271/2007-01-1574.
(25) May, K. R. *J. Aerosol Sci.* **1973**, *4*, 235−243.
(26) Kanazawa, S.; Chang, J. S.; Round, G. F.; Sheng, G.; Ohkubo, T.; Nomoto, Y.; Adachi, T. *Combust. Sci. Technol.* **1998**, *133*, 93−105.
(27) Quici, N.; Vera, M. L.; Choi, H.; Puma, G. L.; Dionysiou, D. D.; Litter, M. I.; Destaillats, H. *Appl. Catal., B* **2010**, *95*, 312−319.
(28) Obradović, B. M.; Sretenović, G. B.; Kuraica, M. M. *J. Hazard. Mater.* **2011**, *185*, 1280−1286.
(29) Griffiths, R. F.; Megson, L. C. *Atmos. Environ.* **1984**, *6*, 1195−1206.
(30) Jeong, J.; Sekiguchi, K.; Lee, W.; Sakamoto, K. *J. Photochem. Photobiol., A* **2005**, *169*, 279−287.
(31) Hinds, W. C. *Aerosol Technology*; John Wiley and Sons: Hoboken, NJ, 1999.
(32) Friedlander, S. K. *Smoke, Dust, Haze Fundamentals of Aerosol Behavior*; John Wiley and Sons: Hoboken, NJ, 1977.
(33) Thomas, D.; Vanderschuren, J. *Ind. Eng. Chem. Res.* **1997**, *36*, 3315−3322.
(34) Liu, Y. X.; Zhang, J. *Ind. Eng. Chem. Res.* **2011**, *50*, 3836−3841.
(35) Baulch, D. L.; Cox, R. A.; Crutzen, P. J.; Hampson, R. F., Jr.; Kerr, J. A.; Troe, J.; Watson, R. T. *J. Phys. Chem. Ref. Data* **1982**, *11*, 327−496.
(36) Szpyrkowicz, L.; Juzzolino, C.; Kaul, S. N. *Water Res.* **2001**, *35*, 2129−2136.
(37) Park, J. Y.; Tomicic, I.; Round, G. F.; Chang, J. S. *J. Phys. D: Appl. Phys.* **1999**, *32*, 1006−1011.
(38) Muruganandham, M.; Swaminathan, M. *Dyes Pigm.* **2004**, *62*, 269−275.